Molecular Pharmacology Fast Forward. Published on February 16, 2010 as doi:10.1124/mol.109.061804
This article has not been copyedited and formatted. The final version may differ from this version.

Functional Characterization of V2-Vasopressin Receptor Substitutions (R137H/C/L) Leading to Nephrogenic Diabetes Insipidus and Nephrogenic Syndrome of Inappropriate Antidiuresis; Implications for treatments.

Moulay D. Rochdi, Gabriel A. Vargas, Eric Carpentier, Geneviève Oligny-Longpré, Stanford Chen, Abraham Kovoor, Stephen E. Gitelman, Stephen M. Rosenthal, Mark von Zastrow and Michel Bouvier*

Institut de Recherche en Immunologie et Cancérologie, Département de Biochimie and Groupe de Recherche Universitaire sur le Médicament, Université de Montréal, Montréal, Québec, H3C 3J7, Canada (M.D.R., E.C., G.O.-L., M.B.); Department of Psychiatry (G.A.V., S.C., A.K., M.vZ), Department Cellular & Molecular Pharmacology (M.vZ), and Department of Pediatrics, Division of Endocrinology (S.E.G., S.M.R.), UCSF, San Francisco, CA, USA

Molecular Pharmacology Fast Forward. Published on February 16, 2010 as DOI: 10.1124/mol.109.061804
This article has not been copyedited and formatted. The final version may differ from this version.

Running Title: Signalling and trafficking of NDI and NSIAD V2R mutations

Corresponding author:

Michel Bouvier

IRIC, Université de Montréal

C.P. 6128 Succursale Centre-Ville

Montréal, QC H3C 3J7

Tel: (514) 343-6319

Fax: (514) 343-6843

e-mail: michel.bouvier@umontreal.ca

Number of text pages: 35
Number of tables: 1
Number of figures: 8
Number of references: 32
Number of words in the *Abstract: 249*
Number of words in the *Introduction: 593*
Number of words in the *Discussion*: 1086

Abbreviations: AVP, arginine vasopressin; AQP2, aquaporin 2 water channel; V2R, V2-vasopressin receptor; GPCR, G protein-coupled receptors; PKA, cAMP-dependent protein kinase; NDI, nephrogenic diabetes insipidus; NSIAD, nephrogenic syndrome of inappropriate antidiuresis; MAPK, mitogen-activated protein kinase; DMEM, Dulbecco's modified Eagle's medium; G418, Geneticin; ERK, extracellular signal-regulated kinase; BRET[1], first generation of bioluminescence resonance energy transfer; HTRF, homogeneous time resolved fluorescence technology; Rluc, Renilla luciferase; EYFP, enhanced yellow fluorescent protein; DynK44A, dominant negative mutant of dynamin, HEK, human embryonic kidney; SDS-PAGE, SDS-polyacrylamide gel electrophoresis, PBS, phosphate-buffered saline; pCREluc, cAMP-responsive luciferase reporter plasmid; WT, wild-type; GIRK, G protein-activated inwardly rectifying potassium channel subunits.

Molecular Pharmacology Fast Forward. Published on February 16, 2010 as DOI: 10.1124/mol.109.061804
This article has not been copyedited and formatted. The final version may differ from this version.

ABSTRACT

Substitution of arginine-137 of the vasopressin type 2 receptor (V2R) for histidine (R137H-V2R) leads to nephrogenic diabetes insipidus (NDI) whereas substitution of the same residue to cysteine or leucine (R137C/L-V2R) causes the nephrogenic syndrome of inappropriate antidiuresis (NSIAD), two diseases with opposite clinical outcomes. Still, the three mutant receptors were shown to share constitutive β-arrestin recruitment and endocytosis, resistance to vasopressin-stimulated cAMP production and MAPK activation as well as compromised cell surface targeting, raising questions about the contribution of these phenomenons to the diseases and their potential treatments. Blocking endocytosis exacerbated the elevated basal cAMP levels promoted by R137C/L-V2R but not the cAMP production elicited by R137H-V2R, demonstrating that substitution of R137 to C/L, but not H, leads to constitutive V2R-stimulated cAMP accumulation that most likely underlies NSIAD. The constitutively elevated endocytosis of R137C/L-V2R attenuates the signalling and most likely reduces the severity of NSIAD whereas the elevated endocytosis of R137H-V2R probably contributes to NDI. The constitutive signalling of R137C/L-V2R was not inhibited by treatment with the V2R inverse agonist SR121463. In contrast, owing to its pharmacological chaperone property, SR121463 increased the R137C/L-V2R maturation and cell surface targeting, leading to a further increase in basal cAMP production thus disqualifying it as a potential treatment for R137C/L-V2R NSIAD patients. However, vasopressin was found to promote β-arrestin/AP2-dependent internalization of R137H/C/L-V2R beyond their already elevated endocytosis levels, raising the possibility that vasopressin could have a therapeutic value for R137C/L NSIAD patients by reducing steady state surface receptor levels, thus lowering basal cAMP production.

Molecular Pharmacology Fast Forward. Published on February 16, 2010 as DOI: 10.1124/mol.109.061804
This article has not been copyedited and formatted. The final version may differ from this version.

INTRODUCTION

The arginine vasopressin (AVP) system plays a crucial role in water homeostasis. AVP is synthesized in the hypothalamus and is released upon increased plasma osmolality, decreased arterial pressure and heart volume reduction (Ball, 2007; Treschan and Peters, 2006). In the distal collecting tubules of the kidney, AVP promotes water reabsorption through the aquaporin 2 water channel (AQP2) by binding to, and activating the vasopressin type 2 receptor (V2R). This receptor, which belongs to the family of G protein-coupled receptors (GPCR), promotes cAMP production through the activation of Gαs and adenylyl cyclase. It has been suggested that the resulting phosphorylation of AQP2 by the cAMP-dependent protein kinase (PKA) promotes its insertion into the apical plasma membrane of the renal collecting duct principal cells, leading to increased water permeability (Ball, 2007; Treschan and Peters, 2006). Renal insensitivity to AVP results in a failure to reabsorb water, leading to excessive water excretion (>30 ml/kg body wt/d for adults) and diluted urine (<250 mmol/kg) causing dehydration and pathological hypernatremia; a disease known as nephrogenic diabetes insipidus (NDI) (Fujiwara and Bichet, 2005). Most NDI cases result from mutations in the V2R gene (*AVPR2*). To date, over 200 NDI-causing mutations in *AVPR2* has been associated with loss-of-function of V2R signalling (Fujiwara and Bichet, 2005; Spanakis et al., 2008). One of these missense mutations, leading to substitution of an arginine to a histidine at position 137 (R137H), was shown to cause loss-of-function of the V2R as a results of a dramatic decrease in cell surface expression induced by both constitutive internalization and intracellular retention of the receptor due to its impaired maturation (Barak et al., 2001; Bernier et al., 2004b). Unexpectedly, Feldman and colleagues (2005) reported that substitution of the same arginine residue by either cysteine or leucine (R137C or R137L) was causing a distinct renal disorder associated with a V2R gain-of-function, leading to excessive water reabsorption, hyponatremia and seizures. This newly described

Molecular Pharmacology Fast Forward. Published on February 16, 2010 as DOI: 10.1124/mol.109.061804
This article has not been copyedited and formatted. The final version may differ from this version.

syndrome was termed nephorgenic syndrome of inappropriate antidiuresis (NSIAD) (Feldman et al., 2005). Characterization of the R137C- and R137L-V2R signalling properties revealed a constitutively elevated basal V2R-promoted cAMP production (Feldman et al., 2005). Although the structural mechanisms involved in GPCRs activation are still incompletely understood, the well conserved $DR^{137}Y/H$ motif is thought to be involved in the intramolecular interactions that stabilize inactive and/or activated conformations of various GPCRs (Rovati et al., 2007).

While previous studies have extensively investigated the loss-of-function R137H-V2R (Barak et al., 2001; Bernier et al., 2004b), only limited data are available for the R137C- and R137L-V2R. Recently, Kocan et al. (2009) reported that, as previously shown for R137H-V2R (Bernier et al., 2004b), R137C- and R137L-V2R promote agonist-independent recruitment of β-arrestin to the receptor and the subsequent internalization of the receptor/β-arrestin complex. Despite this increased constitutive β-arrestin recruitment, which should blunt the Gαs signalling activity, a significant elevated cAMP production was observed. This contrasts with the absence of spontaneous Gαs activation for the R137H substitution and most likely contributes to the opposite pathological outcomes resulting from these different substitutions at position 137. To determine if other functional properties, specific to the R137C- and R137L-V2R, contribute to the gain-of-function associated with these V2R mutants, we characterized multiple functional properties of the R137C- and R137L-V2R by investigating their maturation and cell surface targeting, basal and agonist-stimulated cAMP production and mitogen-activated protein kinase (MAPK) activation as well as their constitutive and ligand-regulated endocytosis. Finally, we investigated the potential therapeutic benefit of using a V2R-specific inverse agonist (SR121463B) on the gain-of-function of the R137C- and R137L-V2R mutant receptors and thus, its suitability as a potential therapeutic agent for NSIAD.

Molecular Pharmacology Fast Forward. Published on February 16, 2010 as DOI: 10.1124/mol.109.061804
This article has not been copyedited and formatted. The final version may differ from this version.

MATERIALS AND METHODS:

Materials. Dulbecco's modified Eagle's medium (DMEM), fetal bovine serum, Geneticin (G418), L-glutamine and penicillin-streptomycin were purchased from Wisent. Fugene6 was obtained from Roche Diagnostics. Coelenterazine-*h* was from Prolume. Poly-D-lysine and 8-arginine-vasopressin (AVP) as well as the antibodies against the FLAG epitope (M1 and M2) were obtained from Sigma-Aldrich Canada. Antibodies recognizing the extracellular signal-regulated kinases (ERK) and their phosphorylated forms (P-ERK) were from Santa Cruz Biotechnology Inc. whereas anti-mouse and anti-rabbit HRP-conjugated IgG were from GE Healthcare. The enhance chemiluminescence lightening substrat was obtained from PerkinElmer. The white opaque and clear bottom 96-well plates were from Corning. The Cy3-conjugated donkey anti-mouse secondary antibody was from Jackson ImmunoResearch. The Mithras LB940 from Berthold was the plate reader used to measure the first generation of bioluminescence resonance energy transfer (BRET^1) while the ARTEMIS TR-FRET microplate reader (Cosmo Bio Co., Ltd) was used to read the homogeneous time resolved fluorescence (HTRF) technology assays in this study.

Plasmid constructs and mutagenesis. A FLAG epitope tagged human V2R was described previously (Klein et al., 2001). FLAG-R137L-V2R, FLAG-R137C-V2R and FLAG-R137H-V2R mutant constructs were generated from the FLAG-WT-V2R using site-directed mutagenesis (QuikChange; Stratagene) according to the manufacturer's instructions in order to replace R137 by the appropriate amino acid. The same strategy was used to generate the enhanced yellow fluorescent protein-tagged (EYFP) mutant V2R using the previously published EYFP-WT V2R (Charest and Bouvier, 2003). The Renilla luciferase tagged β-arrestin2 (β-arrestin2-*R*luc) and the EYFP tagged β2-adaptin (β2-adaptin-EYFP) (Hamdan et al., 2007) as well as the dominant

Molecular Pharmacology Fast Forward. Published on February 16, 2010 as DOI: 10.1124/mol.109.061804
This article has not been copyedited and formatted. The final version may differ from this version.

negative mutant of dynamin (DynK44A) (Rochdi and Parent, 2003) constructs were described previously.

Cell culture and plasmid transfections. Unless otherwise stated, human embryonic kidney (HEK) 293 cells were cultured in high glucose DMEM supplemented with 10% fetal bovine serum, 100 units/ml penicillin-streptomycin, and 2 mM-glutamine at 37°C in a humidified chamber at 95% air and 5% CO_2. For transfections in 6-well plates, $4x10^5$ HEK293 cells were seeded and transfected the next day using Fugene6 according to manufacturer's recommendations.

Measurement of cell surface expression and AVP-induced internalization. Agonist-promoted internalization was assessed as described previously (Rochdi and Parent, 2003) using HEK293 cells transiently expressing the different V2R constructs. Briefly, the culture medium was removed and replaced with DMEM/0.5% bovine serum albumin/20 mM HEPES in the presence or absence of AVP. After 60-min incubation at 37°C, the medium was removed and cells were fixed with Tris-buffered saline/3.7% formaldehyde for 5 min at room temperature. Cell surface expression was measured using an ELISA-based assay and anti-FLAG M2 monoclonal antibody. The percentage of agonist-promoted receptor internalization was determined as follows: (1 – stimulated/unstimulated) x 100.

Total cell extract analysis by western blot. Proteins from total cell lysates were resolved by SDS-polyacrylamide gel electrophoresis (PAGE) before being transferred onto a nitrocellulose membrane. Protein immunodetection on membranes was done using the Anti-FLAG M2 (0.2 µg/ml) antibody.

Molecular Pharmacology Fast Forward. Published on February 16, 2010 as DOI: 10.1124/mol.109.061804
This article has not been copyedited and formatted. The final version may differ from this version.

BRET[1] measurement of β-arrestin2/β2-adaptin interaction. A stable β2-adaptin-EYFP cell line generated as described previously (Hamdan et al., 2007) was transfected with β-arrestin2-*R*luc and either the WT-V2R, R137H-V2R, R137C-V2R or R137L-V2R construct. Approximately 18 h after transfection, cells were detached by trypsinization and seeded (~$5X10^4$ cells/well) into opaque 96-well (white wall, clear bottom) tissue culture plates previously treated with poly-D-lysine, and re-incubated at 37 °C for another 18 h. On the day of the experiment, the culture medium was replaced by phosphate-buffered saline (PBS) and incubated with or without agonist at room temperature for the specified time. To measure the BRET[1] signal, the clear bottom of the 96-well white plate was covered with a white-backed tape adhesive (PerkinElmer Life Sciences), and the BRET[1] substrate for *R*luc, coelenterazine-*h*, was added to all wells (5 μM final concentration), followed by BRET[1] measurement on the Mithras LB940 plate reader, which allows the sequential integration of signals detected in the 480 ± 20 nm and 530 ± 20 nm windows. The BRET[1] signal was calculated as a ratio of the light emitted by EYFP (530 ± 20 nm) over the light emitted by *R*luc (480 ± 20 nm). Total luciferase and EYFP values were comparable in each condition tested.

BRET[1] measurement of β-arrestin recruitment to WT- and mutant V2R. EYFP-tagged WT and mutant V2R were transiently co-expressed with the β-arrestin2-*R*luc in HEK293 cells. Forty eight hours after transfection, cells were detached in PBS and distributed in an opaque 96-wells plate. Cells were then stimulated for 20 min at 37°C with increasing amount of AVP (from 10^{-15} to 10^{-5} M) prior to the addition of coelenterazine-*h* (5 μM final) and BRET measurement using the Mithras LB940 plate reader. Potency values (EC50) of the AVP-promoted β-arrestin

Molecular Pharmacology Fast Forward. Published on February 16, 2010 as DOI: 10.1124/mol.109.061804
This article has not been copyedited and formatted. The final version may differ from this version.

recruitment to the receptors were determined using the GraphPad Prism software (San Diego, CA).

Visualization of receptor localization and internalization by fluorescence Microscopy. FLAG-tagged mutant receptors present at the plasma membrane were specifically labelled with the M1 monoclonal antibody and subsequent internalization was visualized using a minor modification of a method described previously (Gage et al., 2001). Briefly, HEK293 cells stably or transiently expressing the indicated FLAG-tagged receptor constructs were plated on glass coverslips (Corning), and surface receptors were specifically labelled by incubating intact cells with the M1 anti-FLAG monoclonal antibody (2.5 μg/ml; Sigma) at 37°C for 30 min in the absence of agonist. The cells were then incubated (37°C for 30 min) in the presence or absence of 10 μM AVP (Sigma), as indicated. Cells were then fixed for 10 min using 3.7% formaldehyde freshly dissolved in PBS followed by three washes using Tris-buffered saline supplemented with 1 mM $CaCl_2$. Fixed specimens were permeabilized with 0.1% Triton X-100 (Sigma) in Blotto (3% dry milk in Tris-buffered saline with 1 mM $CaCl_2$) and incubated with Cy3-conjugated donkey anti-mouse secondary antibody (1:500 dilution) for 45 min. Fluorescence microscopy was performed using an inverted Nikon Diaphot microscope equipped with a Nikon 60x NA1.4 objective and epifluorescence optics. Images were collected using a 12-bit cooled charge-coupled device camera (Princeton Instruments) interfaced to a Macintosh computer.

cAMP accumulation measurement. cAMP accumulation was measure using the *cAMP dynamic 2* kit (Cisbio, Bedford, MA, USA) according to manufacturer's recommendations. Briefly, HEK293 cells transiently expressing either the WT-V2R, R137H-V2R, R137C-V2R or R137L-V2R were transferred into a 384 well plate ($5x10^4$ cells/well). AVP or vehicle was then

Molecular Pharmacology Fast Forward. Published on February 16, 2010 as DOI: 10.1124/mol.109.061804
This article has not been copyedited and formatted. The final version may differ from this version.

added to the cell suspension followed by 15 min incubation at room temperature. Thereafter, conjugate+lysis buffer as well as d2cAMP where added to each well followed by the addition of the anti-cAMP cryptate antibody. The plate was then incubated at room temperature for one hour and HTRF measured. Results were obtained by calculating the 665/620nm values ratio expressed in Delta F.

Reporter gene assay of cAMP signalling. HEK293 cells were transfected with the WT-V2R or mutant constructs along with the cAMP responsive luciferase reporter plasmid (containing 16 copies of the consensus cAMP response element (Vaisse et al., 2000)) and the *Renilla* luciferase reporter plasmid (pRL-CMV, Promega Corporation, to control for transfection efficiency) using Fugene 6 and according to the manufacturer's protocol. When stable cell lines were used (WT-V2R or R137L-V2R), cells were transfected with only the pCREluc plasmid. Twenty-four hours following transfection, cells were lysed and assayed for luciferase activity using the Dual Luciferase Reporter Assay System (Promega), as previously described (Fluck et al., 2002; Stables et al., 1999). Data are expressed as the mean luciferase activity, in arbitrary units, and normalized to WT-V2R-promoted luciferase activity.

cRNA synthesis, oocyte preparation, injection, and Electrophysiological recording. cDNA-containing plasmids were linearized with the Pvu1 restriction enzyme and used as templates for capped cRNA synthesis using mMESSAGE MACHINE kits (Ambion Corp.). Xenopus oocytes were prepared as described previously (Kovoor et al., 1997) and cRNA was injected (50 nl/oocyte) with a Drummond microinjector. Oocytes were incubated for 48 hr after injection in normal oocyte saline buffer solution (96 mM NaCl, 2 mM KCl, 1 mM $MgCl_2$, 1 mM $CaCl_2$, and 5 mM HEPES, pH 7.5) supplemented with sodium pyruvate (2.5 mM) and gentamycin (50

Molecular Pharmacology Fast Forward. Published on February 16, 2010 as DOI: 10.1124/mol.109.061804
This article has not been copyedited and formatted. The final version may differ from this version.

μg/ml) prior to their transfer to recording buffer (74 mM NaCl, 24 mM KCl, 1 mM $MgCl_2$, 1 mM $CaCl_2$, and 5 mM HEPES, pH 7.5) in order to enhance sensitivity for inward K^+ conductance. For electrophysiological analysis, oocytes were clamped at -80 mV with two electrodes filled with 3 M KCl having resistances of 0.5-1.5 megohm, using a Geneclamp 500 amplifier and pCLAMP 9 software (Axon Instruments). All data were digitally recorded (Digidata, Axon Instruments) and low-pass filtered.

ERK1/2 phosphorylation assay. Cells transiently expressing the different V2R constructs were grown in 6-well plates and rendered quiescent by serum starvation for 16h prior to a 5 min stimulation with 1 μM AVP. Plates were then put on ice and the cells were washed twice with ice-cold PBS and solubilized directly in 150 μl of Laemmli sample buffer containing 50 mM dithiothreitol. The samples were sonicated for 15 sec and heated for 5 min at 95°C prior to SDS-PAGE. ERK1/2 phosphorylation was detected by immunoblotting and chemiluminescence using mouse monoclonal anti-P-ERK and anti-mouse HRP-conjugated antibodies. After densitometric quantification of phosphorylation, membranes were stripped of immunoglobulins and reprobed with a rabbit polyclonal anti-ERK antibody. ERK phosphorylation was normalized according to the protein loads by expressing the data as a ratio of P-ERK over total ERK. Immunoreactivities were determined by densitometric analysis of the films using the Quantity One software (Bio-Rad). Statistical analysis and curve fitting were done using the GraphPad Software (San Diego, CA). Statistical significance of the differences was assessed using one-way analysis of variance and post hoc Bonferroni's test.

Molecular Pharmacology Fast Forward. Published on February 16, 2010 as DOI: 10.1124/mol.109.061804
This article has not been copyedited and formatted. The final version may differ from this version.

RESULTS

Cell surface expression of R137H-, R137C- and R137L-V2R mutants. It has previously been shown that several mutations within the coding sequence of V2R affect the level of receptor cell surface expression (Bichet et al., 1994; Ranadive et al., 2008; Wenkert et al., 1996). In particular, the R137H-V2R has been reported to have low steady state surface expression, owing in part to its constitutive internalization once it reaches the cell surface (Barak et al., 2001; Bernier et al., 2004b; Hamdan et al., 2007). To determine if substitutions of arginine 137 to either leucine or cysteine residues also affect receptor cell surface density, ELISA (enzyme-linked immunosorbent assay) were carried-out on intact HEK293 cells transiently expressing the R137C-, R137L-R137H- and wild type-(WT) V2R bearing a FLAG epitope at the N-terminus to allow immuno-detection. Fig. 1A shows that, compared to the WT-V2R, the R137C and R137L exhibit a ~40% reduction in cell surface expression, which is equivalent to what is observed for the R137H-V2R. The reduced cell surface expression of one of the mutant receptors (R137L-V2R) was further confirmed by radioligand binding experiments using [^{3}H]AVP as the tracer (Supplementary Fig. 1A). Saturable high-affinity binding was observed with both transiently expressing WT-V2R and R137L-V2R cells but significantly lower maximal binding was systematically observed in cells expressing the mutant receptor. Moreover, affinity towards AVP was similar for all V2R constructs, as determined by radio-ligand binding saturation experiments (see Supplementary Table 1).

To determine if, as shown for R137H-V2R, the reduced cell surface expression of the R137C- and R137L-V2R results from constitutive internalization, we quantitatively assessed the effect of a dynamin dominant negative mutant, DynK44A, that has been shown to inhibit both constitutive and agonist-induced internalization by preventing the pinching-off of the endocytic vesicles without preventing the assembly of the internalization machinery (Damke et al., 1994; Hamdan et

Molecular Pharmacology Fast Forward. Published on February 16, 2010 as DOI: 10.1124/mol.109.061804
This article has not been copyedited and formatted. The final version may differ from this version.

al., 2007). As shown in Fig. 1A, co-transfecting DynK44A modestly increased the cell surface expression of the WT receptor (by less than 10%) whereas surface expression of R137H, R137C and R137L-V2R increased by 48%, 29% and 40%, respectively, indicating that constitutive endocytosis is involved in the reduced steady state cell surface expression of the three mutants.

To explore further the mechanism underlying the constitutive endocytosis, we took advantage of the recently developed BRET-based assay, monitoring the interaction between β-arrestin2 and the β2 subunit of the clathrin adaptor AP-2 (β2-adaptin) (Hamdan et al., 2007). The basal BRET between β2-adaptin-EYFP and β-arrestin2-luciferase was significantly higher in cells transiently expressing the R137C-, R137L- or R137H-V2R when compared to cells expressing the WT-V2R (Fig. 1B), indicating that the mutant receptors constitutively promote the assembly of the β-arrestin2/AP2 complex resulting into spontaneous endocytosis. In all cases, inhibition of this spontaneous endocytosis with DynK44A led to a significant increase of the BRET signal, reflecting the accumulation of the receptor/β-arrestin/AP2 complex in the unsevered endocytotic vesicles (Fig. 1B).

Agonist-promoted internalization of R137H-, R137C- and R137L-V2R. In order to investigate if, in addition to their constitutive internalization, the R137C-, R137L- and R137H-V2R could still undergo agonist-promoted internalization, immunofluorescence microscopy, cell surface ELISA, and β-arrestin2/AP2 BRET experiments were performed on transiently expressing cells, in the presence or absence of AVP stimulation. As shown in Fig. 2A, the WT-V2R is located almost exclusively at the cell surface in the absence of AVP stimulation, while the R137C-, R137L- and R137H-V2R are seen in intracellular vesicles, confirming their constitutive endocytosis. AVP treatment (10 μM) led to a massive redistribution of the WT-V2R from the

Molecular Pharmacology Fast Forward. Published on February 16, 2010 as DOI: 10.1124/mol.109.061804
This article has not been copyedited and formatted. The final version may differ from this version.

plasma membrane into endocytic vesicles and promoted additional endocytosis of the mutant receptors. The ability of the mutant receptors to undergo agonist-promoted endocytosis despite their already high level of spontaneous endocytosis was further confirmed and quantified by cell surface ELISA (Fig. 2B). Similarly, although the β-arrestin2/AP2 BRET signal was already elevated for the three mutant receptors, 1 μM AVP further increased the BRET signal (Fig. 2C), indicating that hormone binding promotes additional engagement of the endocytic machinery. Such agonist-promoted engagement of the endocytic machinery by the mutant receptors was further confirmed by performing dose-response curves of β-arrestin2 recruitment directly to the receptors by BRET using transiently expressed EYFP-tagged versions of the WT-, R137H-, R137C- and R137L-V2R, in combination with the *R*luc-tagged β-arrestin construct (Table 1). The results show that the EC50 values are similar for all receptors, confirming that the mutations do not affect the affinity for AVP or the ability of the AVP-bound receptors to recruit β-arrestin2.

Signalling properties of the R137C and R137L-V2R mutants. It has been previously shown that the R137H substitution causes a loss of AVP-induced cAMP production (Barak et al., 2001; Bernier et al., 2004b). For the R137L- and R137C-V2R, which were shown to promote elevated basal cAMP production, no information is available about the AVP-stimulated response. Basal and AVP-stimulated cAMP production was therefore investigated in cells transiently expressing the WT, R137H-, R137L or R137C-V2R. Whether measured using a cAMP-responsive reporter gene assay (CRE-luciferase) (Fig. 3A), or a FRET-based cAMP immune-detection assay (Fig. 3B), an elevated basal cAMP production was observed for both R137L- or R137C-V2R compared to WT-V2R, confirming their increased constitutive activity towards the cAMP production pathway. The higher basal cAMP production promoted by the R137C- and R137L-

Molecular Pharmacology Fast Forward. Published on February 16, 2010 as DOI: 10.1124/mol.109.061804
This article has not been copyedited and formatted. The final version may differ from this version.

V2R was further exacerbated when preventing their internalization with DynK44A (Fig. 3B), suggesting that the manifestation of their constitutive activity is dampened by their concomitant endocytosis. The elevated basal cAMP levels observed did not result from different expression levels since clonal populations of cells stably expressing similar number of WT- and R137L-V2R (Supplementary Fig. 2 and Supplementary Table 1) confirmed that R137L-V2R promotes significantly higher cAMP production than its WT counterpart (Fig. 3C). It should be noted that, as was observed in transiently expressing cells, the affinity for [^{3}H]AVP was the same for the WT and mutant form of the receptor (Supplementary Table 1). Despite the elevated basal activity observed in cells transiently expressing R137L- and R137C-V2R, no further increase in cAMP production could be detected following 1 μM AVP stimulation (Fig. 4A); a loss of responsiveness that was also observed for the R137H-V2R. These results were further confirmed using the highly sensitive CRE-luciferase reporter gene assay in cells stably expressing the same level of WT- and R137L-V2R (see Supplementary Fig 2). Although the R137L-V2R basal activity was higher than the WT-V2R, no increase in luciferase activity could be observed after a 24 hours stimulation with 1 μM AVP in cells expressing R137L-V2R whereas a 6-fold increase was observed in cells expressing the WT receptor (Fig. 4B).

The loss of AVP-promoted Gαs pathway activation by V2R was further confirmed for the R137L mutant by monitoring GIRK channel activation in frog oocytes co-expressing Gαs and the G protein-activated inwardly rectifying potassium channel subunits (GIRK1 and GIRK4) (Kovoor et al., 1997; Lim et al., 1995). As shown in Fig. 4C, 1 μM AVP stimulation induced a robust inward current in oocytes expressing the WT-V2R while no response was detected in R137L-V2R expressing oocytes.

Molecular Pharmacology Fast Forward. Published on February 16, 2010 as DOI: 10.1124/mol.109.061804
This article has not been copyedited and formatted. The final version may differ from this version.

AVP binding to V2R has been shown to promote activation of the extracellular signal-regulated kinase (ERK1/2) (Pequeux et al., 2004). To assess whether substitution of R137 for C, L or H could also affect this signalling pathway, AVP-promoted ERK1/2 phosphorylation was measured in transiently expressing V2R cells. As expected, the WT-V2R receptor induced a robust ERK1/2 phosphorylation upon 1 μM AVP stimulation whereas no AVP-induced phosphorylation of ERK1/2 was observed in cells expressing R137H-, R137C- or R137L-V2R (Fig. 5), indicating that the loss of AVP responsiveness is not limited to the cAMP production pathway.

Although elevated constitutive endocytosis and loss of both AVP-stimulated cAMP production and ERK1/2 activation are shared by R137H-, R137C- and R137L-V2R, the increased basal cAMP production promoted by R137L- and R137C-V2R was not observed for R137H-V2R, whether constitutive endocytosis was blocked or not (Fig. 3A and B), revealing at least one intrinsic difference (constitutive activity toward the cAMP pathway) between the R137 substitutions causing NDI vs NSIAD.

Maturation and pharmacological chaperoning of R137H-, R137C- and R137L-V2R. The R137H-V2R mutant has previously been shown to have impaired folding, leading to a decrease expression of the mature form of the receptor as monitored by its glycosylation state (Morello and Bichet, 2001). Such impaired maturation was partially corrected by sustained treatment with selective lipophilic ligands acting as pharmacological chaperones (Bernier et al., 2004a; Bernier et al., 2004b; Morello et al., 2000)**.** To determine if these properties are shared by R137L- and R137C-V2R, we assessed their maturation profiles in transiently expressing cells, in the absence and presence of the pharmacological chaperone SR121463. Our results show that, similarly to the

Molecular Pharmacology Fast Forward. Published on February 16, 2010 as DOI: 10.1124/mol.109.061804
This article has not been copyedited and formatted. The final version may differ from this version.

NDI-associated R137H-V2R, the NSIAD-causing R137C and R137L substitutions affect receptor maturation, as indicated by a reduction of the fully glycosylated form (~50kDa) of the three mutant receptors compared to the WT (Fig. 6). Similarly to what was observed for R137H-V2R, the SR121463 treatment (10 μM) favoured maturation of R137C- and R137L-V2R, as revealed by the marked increase of the fully glycosylated form of the receptor.

Effect of V2R-specific inverse agonist on the constitutive signalling of R137C and R137L-V2R mutants. It has previously been shown that, in addition to its pharmacological chaperone property, the V2R antagonist SR121463 is endowed with inverse agonist activity toward the artificially designed constitutively active mutant D136A-V2R (Morin et al., 1998). We therefore assessed the ability of this compound to silence the constitutive activity of transiently expressed R137C- and R137L-V2R. Fig. 7A shows that a short term (30 min) treatment with 10 μM SR121463 did not affect the elevated basal cAMP production promoted by R137C and R137L, indicating that SR121463 does not act as an inverse agonist on these mutants. Longer term (16h) treatment with SR121463 also did not reveal any inverse agonist effects. In fact, it potentiated the elevated basal cAMP accumulation observed in cells expressing R137C- and R137L-V2R. This potentiating effect is most likely due to the increased number of constitutively active receptor at the cell surface, due to the pharmacological chaperone property of SR121463 (Fig. 6).

Since R137H, R137C- and R137L-V2R were all found to promote constitutive association of β-arrestin2 with AP2, leading to the internalization of the receptor (Fig. 2B), we assessed whether it could be blocked by SR121463. As shown in Fig. 7B, the elevated BRET between β-arrestin2-*R*luc and β2-adaptin-EYFP promoted by the transient expression of the three mutant receptors was not reduced upon SR121463 treatment. In fact, the treatment tended to increase the BRET

Molecular Pharmacology Fast Forward. Published on February 16, 2010 as DOI: 10.1124/mol.109.061804
This article has not been copyedited and formatted. The final version may differ from this version.

signal promoted by the receptors most likely, again, as a result of the SR121463-promoted elevation of cell surface receptor number.

Combined effects of misfolding and constitutive internalization on the constitutive activity of the R137C- and R137L-V2R mutants. Our results show that both constitutive internalization and partial intracellular retention of the NSIAD-causing R137C-and R137L-V2R contribute to lower cell surface receptor levels. Together, these two phenomena should therefore reduce the extent of constitutive activity detected in cells expressing the NSIAD-causing mutant receptors. To test this hypothesis, we assessed the effect of inhibiting receptor endocytosis (using DynK44A co-transfection) in combination with increasing receptor targeting to the cell surface (using 10 μM SR121463) on basal cAMP production. As shown in Fig. 8, the combined over-expression of DynK44A and long term SR121463 treatment resulted in an additive increase in cAMP accumulation in HEK293 cells expressing the R137C- or R137L-V2 receptors but not in cells expressing either the R137H- or the WT-V2 receptors.

Molecular Pharmacology Fast Forward. Published on February 16, 2010 as DOI: 10.1124/mol.109.061804
This article has not been copyedited and formatted. The final version may differ from this version.

DISCUSSION

Our characterization of the molecular defects of NSIAD-causing mutant R137L- and R137C-V2R has revealed a high degree of similarity with the previously described NDI-causing mutant R137H-V2R. First, the three mutant receptors were shown to undergo elevated constitutive endocytosis, as revealed by a considerably reduced steady state cell surface level that could be partly normalized by inhibiting constitutive internalization. These results are consistent with a recent study reporting that the three receptors were constitutively localized in intra-cellular vesicles (Kocan et al., 2009). For the three mutant receptors, our results show that the elevated endocytosis arrises from the same mechanism involving the constitutive engagement of the clathrin-dependent pathway, as revealed by the increased basal BRET observed between β-arrestin2 and β2-adaptin. These results are in agreement with previous reports demonstrating that R137H-V2R, as well as R137L- and R137C-V2R spontaneously recruit β-arrestin2 in the absence of agonist stimulation (Bernier et al., 2004b; Kocan et al., 2009). Despite their constitutive internalization, the three mutant receptors can still recruit β-arrestin and engage the β-arrestin2/AP2 complex upon AVP stimulation, leading to additional internalization. These results indicate that the substitutions only partially mimic or stabilize the receptor conformation recruiting the endocytic machinery.

The three mutant receptors also shared altered maturation, as revealed by a decreased proportion of the fully glycosylated form of the receptors, indicative of reduced Golgi processing. This altered processing is also revealed by the ability of pharmacological chaperones to promote receptor maturation and cell surface targeting. These results contrast with the recent suggestion, based on qualitative immunofuorescence analyses, that R137C- and R137L-V2R forward trafficking is not impaired and that their constitutive endocytosis is solely responsible for the

Molecular Pharmacology Fast Forward. Published on February 16, 2010 as DOI: 10.1124/mol.109.061804
This article has not been copyedited and formatted. The final version may differ from this version.

decreased cell surface expression (Kocan et al., 2009). The authors concluded that this represents a major difference between R137H-V2R on one hand and R137C- and R137L-V2R on the other. In contrast, our results show that both impaired maturation and elevated constitutive endocytosis contribute to the reduced steady state cell surface expression of R137C- and R137L- as well as R137H-V2R. Consistent with this notion, inhibition of endocytosis only partially restored cell surface expression of the three mutant receptors.

An additional characteristic shared by the three mutants is their inability to promote both cAMP production and ERK1/2 activation upon AVP stimulation, indicating a common loss of functional responsiveness. One cannot exclude that the mutant receptors could allow a weak agonist-promoted Gαs signalling that fell below the detection threshold. However, this is unlikely since no AVP-stimulated cAMP production could be observed for R137L, even when the highly amplified CRE-Luc reporter assay was used. The loss of responsiveness does not originate from a loss of AVP binding to the receptor since AVP affinity, as determined by radio-ligand binding studies, were similar for all receptors studied and, as indicated above, AVP-induced recruitment of the endocytic machinery and subsequent endocytosis was observed for all mutant receptors. The fact that AVP is able to promote internalization but is unable to stimulate detectable cAMP production or ERK1/2 activation suggests that the active conformation required for β-arrestin2 and downstream endocytic effectors recruitment are different from those leading to Gαs and ERK1/2 activation.

The only difference observed between the loss-of-function R137H mutant and the two gain-of-function mutants R137C- and R137L-V2R resides in their basal constitutive activity toward the cAMP pathway. Indeed, whereas R137H-V2R basal activity is undistinguishable from that of the

Molecular Pharmacology Fast Forward. Published on February 16, 2010 as DOI: 10.1124/mol.109.061804
This article has not been copyedited and formatted. The final version may differ from this version.

WT-receptor, R137C- and R137L-V2R promoted higher basal cAMP levels in accordance with what we previously reported (Feldman et al., 2005).

Interestingly, the elevated basal activity of the R137C and R137L-V2R was observed despite the constitutive recruitment of β-arrestin2, known to abrogate receptor-promoted Gαs signalling (Barki-Harrington and Rockman, 2008). This raises the intriguing possibility that the balance between the constitutive engagement of Gαs and β-arrestin2 may determine the extent of basal cAMP production and may explain the difference between the NSIAD and NDI-causing mutations described herein.

Inverse agonists have recently emerged as a group of bioactive compounds that can bind to constitutively active receptors and reduce their basal signalling (Rodriguez-Puertas and Barreda-Gomez, 2006) and thus could represent a potential therapeutic avenue. The inverse agonist SR121463, which was shown to reduce the constitutive cAMP production promoted by the artificially designed D136A-V2R, was however unable to silence the constitutive activity of R137C- and R137L-V2R. In fact, the effect of the compound increased basal cAMP level promoted by the receptors, most likely as a consequence of the increased receptor number reaching the cell surface due to its pharmacological chaperone action. The lack of inverse agonist effect of SR121463 on the R137C- and R137L-V2R-promoted cAMP production is consistent with the absence of therapeutic activity in hyponatremic NSIAD patients carrying the mutation leading to the R137C substitution in their *AVPR2* gene (Decaux et al., 2007). At the mechanistic level, the inability of SR121463 to silence the constitutive activity of R137C- and R137L-V2R suggests that the structural changes causing the constitutive activation of the mutant receptors cannot be reversed by the inverse agonist binding. Although less likely, the resistance of the spontaneous activity to the inhibitory action of SR121463 could indicate that the elevated cAMP

Molecular Pharmacology Fast Forward. Published on February 16, 2010 as DOI: 10.1124/mol.109.061804
This article has not been copyedited and formatted. The final version may differ from this version.

production could result from the increased expression or activation of another Gαs or adenylyl cyclase-activating protein as a result of the expression of the mutant V2R.

Although inactive for treating NSIAD patients harbouring the R137C and R137L substitutions, the pharmacological chaperone properties of SR121463 made it an effective treatment for NDI patients carrying R137H-V2R (Bernier et al., 2006). In contrast, the ideal compound to treat NSIAD would have inverse agonist efficacy toward the cAMP pathway while lacking pharmacological chaperone activity. Thus screening for such ligands, using R137C and R137L-V2R expressing cells, would be a rational approach for the discovery of a NSIAD treatment. Reducing cell surface expression of the receptor by either inhibiting receptor targeting to the cell surface or promoting its endocytosis could also represent alternative therapeutic avenues since reduced steady state surface receptor levels would result in lower basal cAMP production. AVP administration could represent such a therapeutic avenue for these patients since we found that AVP promoted a reduction in cell surface receptor without activating the cAMP or the ERK1/2 pathways.

In conclusion, our study shows that, although they lead to some common receptor anomalies, distinct substitutions occurring at a same position also have distinct consequences that are responsible for the opposite clinical outcomes observed for R137H vs R137L/C. This illustrates the importance of a detailed characterization of the functional consequences of receptor mutants in order to understand the molecular basis of the disease and to provide clues for the development of therapeutic avenues.

Molecular Pharmacology Fast Forward. Published on February 16, 2010 as DOI: 10.1124/mol.109.061804
This article has not been copyedited and formatted. The final version may differ from this version.

ACKNOWLEDGEMENTS:

We would like to thank Monique Lagacé for valuable insights and thorough reading of the manuscript.

Molecular Pharmacology Fast Forward. Published on February 16, 2010 as DOI: 10.1124/mol.109.061804
This article has not been copyedited and formatted. The final version may differ from this version.

Molecular Pharmacology Fast Forward. Published on February 16, 2010 as DOI: 10.1124/mol.109.061804
This article has not been copyedited and formatted. The final version may differ from this version.

REFERENCES:

Ball SG (2007) Vasopressin and disorders of water balance: the physiology and pathophysiology of vasopressin. *Ann Clin Biochem* **44**(Pt 5):417-431.

Barak LS, Oakley RH, Laporte SA and Caron MG (2001) Constitutive arrestin-mediated desensitization of a human vasopressin receptor mutant associated with nephrogenic diabetes insipidus. *Proc Natl Acad Sci U S A* **98**(1):93-98.

Barki-Harrington L and Rockman HA (2008) Beta-arrestins: multifunctional cellular mediators. *Physiology (Bethesda)* **23**:17-22.

Bernier V, Bichet DG and Bouvier M (2004a) Pharmacological chaperone action on G-protein-coupled receptors. *Curr Opin Pharmacol* **4**(5):528-533.

Bernier V, Lagace M, Lonergan M, Arthus MF, Bichet DG and Bouvier M (2004b) Functional rescue of the constitutively internalized V2 vasopressin receptor mutant R137H by the pharmacological chaperone action of SR49059. *Mol Endocrinol* **18**(8):2074-2084.

Bernier V, Morello JP, Zarruk A, Debrand N, Salahpour A, Lonergan M, Arthus MF, Laperriere A, Brouard R, Bouvier M and Bichet DG (2006) Pharmacologic chaperones as a potential treatment for X-linked nephrogenic diabetes insipidus. *J Am Soc Nephrol* **17**(1):232-243.

Bichet DG, Birnbaumer M, Lonergan M, Arthus MF, Rosenthal W, Goodyer P, Nivet H, Benoit S, Giampietro P, Simonetti S and et al. (1994) Nature and recurrence of AVPR2 mutations in X-linked nephrogenic diabetes insipidus. *Am J Hum Genet* **55**(2):278-286.

Charest PG and Bouvier M (2003) Palmitoylation of the V2 vasopressin receptor carboxyl tail enhances beta-arrestin recruitment leading to efficient receptor endocytosis and ERK1/2 activation. *J Biol Chem* **278**(42):41541-41551.

Damke H, Baba T, Warnock DE and Schmid SL (1994) Induction of mutant dynamin specifically blocks endocytic coated vesicle formation. *J Cell Biol* **127**(4):915-934.

Decaux G, Vandergheynst F, Bouko Y, Parma J, Vassart G and Vilain C (2007) Nephrogenic syndrome of inappropriate antidiuresis in adults: high phenotypic variability in men and women from a large pedigree. *J Am Soc Nephrol* **18**(2):606-612.

Feldman BJ, Rosenthal SM, Vargas GA, Fenwick RG, Huang EA, Matsuda-Abedini M, Lustig RH, Mathias RS, Portale AA, Miller WL and Gitelman SE (2005) Nephrogenic syndrome of inappropriate antidiuresis. *N Engl J Med* **352**(18):1884-1890.

Fluck CE, Martens JW, Conte FA and Miller WL (2002) Clinical, genetic, and functional characterization of adrenocorticotropin receptor mutations using a novel receptor assay. *J Clin Endocrinol Metab* **87**(9):4318-4323.

Fujiwara TM and Bichet DG (2005) Molecular biology of hereditary diabetes insipidus. *J Am Soc Nephrol* **16**(10):2836-2846.

Gage RM, Kim KA, Cao TT and von Zastrow M (2001) A transplantable sorting signal that is sufficient to mediate rapid recycling of G protein-coupled receptors. *J Biol Chem* **276**(48):44712-44720.

Hamdan FF, Rochdi MD, Breton B, Fessart D, Michaud DE, Charest PG, Laporte SA and Bouvier M (2007) Unraveling G protein-coupled receptor endocytosis pathways using real-time monitoring of agonist-promoted interaction between beta-arrestins and AP-2. *J Biol Chem* **282**(40):29089-29100.

Klein U, Muller C, Chu P, Birnbaumer M and von Zastrow M (2001) Heterologous inhibition of G protein-coupled receptor endocytosis mediated by receptor-specific trafficking of beta-arrestins. *J Biol Chem* **276**(20):17442-17447.

Kocan M, See HB, Sampaio NG, Eidne KA, Feldman BJ and Pfleger KD (2009) Agonist-independent interactions between beta-arrestins and mutant vasopressin type II receptors associated with nephrogenic syndrome of inappropriate antidiuresis. *Mol Endocrinol* **23**(4):559-571.

Kovoor A, Nappey V, Kieffer BL and Chavkin C (1997) Mu and delta opioid receptors are differentially desensitized by the coexpression of beta-adrenergic receptor kinase 2 and beta-arrestin 2 in xenopus oocytes. *J Biol Chem* **272**(44):27605-27611.

Lim NF, Dascal N, Labarca C, Davidson N and Lester HA (1995) A G protein-gated K channel is activated via beta 2-adrenergic receptors and G beta gamma subunits in Xenopus oocytes. *J Gen Physiol* **105**(3):421-439.

Morello JP and Bichet DG (2001) Nephrogenic diabetes insipidus. *Annu Rev Physiol* **63**:607-630.

Morello JP, Salahpour A, Laperriere A, Bernier V, Arthus MF, Lonergan M, Petaja-Repo U, Angers S, Morin D, Bichet DG and Bouvier M (2000) Pharmacological chaperones rescue cell-surface expression and function of misfolded V2 vasopressin receptor mutants. *J Clin Invest* **105**(7):887-895.

Morin D, Cotte N, Balestre MN, Mouillac B, Manning M, Breton C and Barberis C (1998) The D136A mutation of the V2 vasopressin receptor induces a constitutive activity which permits discrimination between antagonists with partial agonist and inverse agonist activities. *FEBS Lett* **441**(3):470-475.

Pequeux C, Keegan BP, Hagelstein MT, Geenen V, Legros JJ and North WG (2004) Oxytocin- and vasopressin-induced growth of human small-cell lung cancer is mediated by the mitogen-activated protein kinase pathway. *Endocr Relat Cancer* **11**(4):871-885.

Ranadive SA, Ersoy B, Favre H, Cheung CC, Rosenthal SM, Miller WL and Vaisse C (2008) Identification, characterization and rescue of a novel vasopressin-2 receptor mutation causing nephrogenic diabetes insipidus. *Clin Endocrinol (Oxf)*.

Rochdi MD and Parent JL (2003) Galphaq-coupled receptor internalization specifically induced by Galphaq signaling. Regulation by EBP50. *J Biol Chem* **278**(20):17827-17837.

Rodriguez-Puertas R and Barreda-Gomez G (2006) Development of new drugs that act through membrane receptors and involve an action of inverse agonism. *Recent Patents CNS Drug Discov* **1**(2):207-217.

Rovati GE, Capra V and Neubig RR (2007) The highly conserved DRY motif of class A G protein-coupled receptors: beyond the ground state. *Mol Pharmacol* **71**(4):959-964.

Spanakis E, Milord E and Gragnoli C (2008) AVPR2 variants and mutations in nephrogenic diabetes insipidus: review and missense mutation significance. *J Cell Physiol* **217**(3):605-617.

Stables J, Scott S, Brown S, Roelant C, Burns D, Lee MG and Rees S (1999) Development of a dual glow-signal firefly and Renilla luciferase assay reagent for the analysis of G-protein coupled receptor signalling. *J Recept Signal Transduct Res* **19**(1-4):395-410.

Treschan TA and Peters J (2006) The vasopressin system: physiology and clinical strategies. *Anesthesiology* **105**(3):599-612; quiz 639-540.

Vaisse C, Clement K, Durand E, Hercberg S, Guy-Grand B and Froguel P (2000) Melanocortin-4 receptor mutations are a frequent and heterogeneous cause of morbid obesity. *J Clin Invest* **106**(2):253-262.

Wenkert D, Schoneberg T, Merendino JJ, Jr., Rodriguez Pena MS, Vinitsky R, Goldsmith PK, Wess J and Spiegel AM (1996) Functional characterization of five V2 vasopressin receptor gene mutations. *Mol Cell Endocrinol* **124**(1-2):43-50.

Footnotes:

This work was supported by research grants from the National Institute of Health [Grant 1 K08 MH68691-01] and the Kidney Foundation of Canada as well as studentships, fellowships and awards from the Canadian Institute of Health Research; the National Institute of Health training grant [1 K08 MH68691-01]; the Fond de la Recherche en Santé du Québec and the Canada Research Chair in Signal Transduction and Molecular Pharmacology.

Molecular Pharmacology Fast Forward. Published on February 16, 2010 as DOI: 10.1124/mol.109.061804
This article has not been copyedited and formatted. The final version may differ from this version.

FIGURE LEGENDS

Fig. 1. Cell surface expression of the WT-, R137H-, R137C- and R137L-V2R and their constitutive internalization. A, HEK293 cells, transiently expressing the indicated V2R constructs along with the over-expression of DynK44A or an empty vector (pcDNA3), were assessed for receptor surface expression by ELISA using an anti-FLAG antibody, as described in *Material and Methods*. **B,** HEK293 cells stably expressing the β2-adaptin-EYFP subunit of the AP2 complex were transfected with the indicated V2R constructs and β-arrestin2-*R*luc, with or without DynK44A over-expression. β-arrestin2 and AP2 interaction was monitored by BRET. Data shown are the mean ± S.E.M. of three to five independent experiments. Statistical significance of the difference was assessed using paired Student's *t* test. *** $p<0.001$; ** $p<0.01$.

Fig. 2. Agonist-induced internalization of wild-type and mutant V2R assessed by fluorescence microscopy, cell surface ELISA and BRET assays. A, HEK293 cells transiently expressing the FLAG-tagged WT-V2R (panels a, b), R137L-V2R (c, d), R137C-V2R (e, f) or R137H-V2R (g, h) were surface-labelled with anti-FLAG monoclonal antibody as described in *Materials and Methods* and incubated in the absence (a, c, e, g) or presence (b, d, f, h) of 10 μM AVP for 30 minutes prior to fixation. Representative epifluorescence images are shown. **B,** HEK293 cells were transfected with the indicated constructs and receptor internalization was determined by measuring cell surface receptor expression following the incubation of the transfected cells in the absence or presence of AVP (1 μM) using the cell surface ELISA assay and anti-FLAG antibody. **C,** HEK293 cells stably expressing the EYFP-fused β2-adaptin subunit of the AP2 complex were transfected with the indicated V2R constructs and β-arrestin2-*R*luc.

Molecular Pharmacology Fast Forward. Published on February 16, 2010 as DOI: 10.1124/mol.109.061804
This article has not been copyedited and formatted. The final version may differ from this version.

BRET[1] measurements of the β-arrestin2/AP2 biosensor were done after 20 min incubation with or without AVP (1 μM). Data shown are the mean ± S.E.M. of three to five independent experiments. Statistical significance of the difference was assessed using paired Student's *t* test. *** $p<0.001$. One-way ANOVA analysis of variance combined with Tukey's multiple comparison test was also performed. ¤¤ $p<0.01$.

Fig. 3. Constitutive cAMP signalling of the mutant V2Rs. A, HEK293 cells were co-transfected with the indicated V2R and the CRE-luciferase reporter constructs, and lysates were assayed for luciferase 24 hours later. In each experiment, reporter gene activity was measured in three replicate wells and the average value from cells expressing R137L-, R137C- or R137H-V2R mutant was normalized to the average value from cells expressing WT-V2R. The bars indicate the mean of normalized luciferase activity across three independent experiments. **B,** HEK293 cells were co-transfected with the indicated receptors and either the DynK44A construct or a control plasmid (pcDNA3). cAMP production was measured using a HTRF-based technology as described in *Material and Methods.* **C,** Stably transfected HEK293 cell clones expressing FLAG-tagged WT- or R137L-V2R, that were matched for receptor expression (see Supplementary Fig 2), were transfected with the CRE-luciferase reporter construct and lysates were assayed for luciferase activity 24 hours later. In each experiment, reporter gene activity was measured in three replicate wells and the average value from cells expressing R137L-V2R mutant was normalized to the average value from cells expressing WT-V2R. Data shown are the mean ± S.E.M. of three to five independent experiments. Statistical significance of the difference was assessed using paired Student's *t* test. *** $p<0.001$; * $p<0.05$. One-way ANOVA analysis of

Molecular Pharmacology Fast Forward. Published on February 16, 2010 as DOI: 10.1124/mol.109.061804
This article has not been copyedited and formatted. The final version may differ from this version.

variance combined with Tukey's multiple comparison test was also performed. ¤¤ $p<0.01$; ¤ $p<0.05$.

Fig. 4. AVP-dependent signalling and G protein coupling estimated by cAMP production measurement and potassium channel currents in oocytes. A, HEK293 cells were transfected with WT or mutant V2R constructs, as indicated. Agonist-induced cAMP production was assessed after 15 min incubation in the presence or absence of AVP (1 μM) using a HTRF-based method, as described in *Material and Methods*. **B**, HEK293 cells stably expressing the indicated V2R were transfected with the CRE-luciferase reporter construct, incubated in the absence or presence of 1 μM AVP for 24 hours, and lysed for luciferase activity measurements. In each experiment, triplicate wells were assayed for each condition and the luminescence units measured from AVP-exposed cells were normalized to the WT-V2R expressing cells not exposed to AVP. Data shown are the mean ± SEM from three independent experiments. **C**, Oocytes were injected with 4ng cRNA of either WT-V2R or the R137L-V2R mutant along with 1ng each of Gαs, GIRK1 and GIRK4 cRNA. Current amplitude produced by the application of AVP was then measured. The inset shows a representative trace of AVP evoked current in an oocyte injected with either WT-V2R cRNA (thick grey trace) or mutant R137L-V2R cRNA (thin black trace). The horizontal bar above the traces indicates AVP application. Data shown are the mean ± S.E.M. of three to five independent experiments. Statistical significance of the difference was assessed using one-way ANOVA analysis of variance combined with Tukey's multiple comparison test. ¤¤ $p<0.01$.

Molecular Pharmacology Fast Forward. Published on February 16, 2010 as DOI: 10.1124/mol.109.061804
This article has not been copyedited and formatted. The final version may differ from this version.

Fig. 5. V2R-promoted MAPK activation. AVP-induced MAPK activation was assessed in HEK293 cells transfected with the indicated V2R constructs. Following 5 min incubation in the presence (+) or absence (-) of AVP (1 μM), cells were lysed in Laemmli sample buffer and extracts resolved by SDS-PAGE. MAPK activity was detected by Western blot using a phospho-specific anti-ERK1/2 antibody (P-ERK1/2). Expression level of ERK1/2 was controlled using an antibody directed against the total kinase population (ERK1/2). Data are expressed as the percentage of P-ERK/ERK of the level observed for AVP-stimulated WT-V2R conditions. Data represent the mean ± S.E.M. of at least three independent experiments. The western blot shown is representative of three independent experiments.

Fig. 6. Effects of the R137C-, R137L-V2R substitutions on receptor maturation profile. HEK293 cells transfected with the indicated receptors were incubated in the absence (upper panel) or presence (lower panel) of SR121463 (10 μM) for 16 hours. Cells extracts were then resolved by SDS-PAGE and receptors visualized by western blotting using an anti-FLAG antibody. Filled arrow (►) shows the fully glycosylated mature form of V2R. Data shown are representative of three to four experiments.

Fig. 7. Effect of V2R inverse agonist SR121463 on the constitutive cAMP production and constitutive endocytosis promoted by the R137C- and R137L-V2R. A, HEK293 cells were transfected with the indicated constructs. Forty-eight hours later, cells were incubated for another 16 hours in the absence or presence of SR121463 (10 μM) and basal cAMP production was measured using a HTRF-based technology, as described in *Material and Methods*. **B,** HEK293 cells stably expressing β2-adaptin-EYFP were transfected with the β-arrestin2-*R*luc and the

Molecular Pharmacology Fast Forward. Published on February 16, 2010 as DOI: 10.1124/mol.109.061804
This article has not been copyedited and formatted. The final version may differ from this version.

indicated receptor constructs. Cells were subsequently incubated for 16 hrs in the presence or absence of SR121463 (10 μM) and BRET[1] measured as described in *Material and Methods*.

Fig. 8. Combined effects of misfolding and constitutive internalization on the constitutive activity of the R137C- and R137L-V2R. HEK293 cells were transfected with the indicated V2R construct and either DynK44A or a control plasmid. Cells were then incubated in the presence or absence of SR121463 (10 μM) for 16 hours and basal cAMP production was measurement using a HTRF-based technology. Data shown are the mean ± S.E.M. of three to five independent experiments. Statistical significance of the difference was assessed using paired Student's *t* test. *** $p<0.001$; ** $p<0.01$. One-way ANOVA analysis of variance combined with the Tukey's multiple comparison test was also performed. ¤¤¤$p<0.001$; ¤¤ $p<0.01$.

Molecular Pharmacology Fast Forward. Published on February 16, 2010 as DOI: 10.1124/mol.109.061804
This article has not been copyedited and formatted. The final version may differ from this version.

Table 1: AVP-induced β-arrestin2 recruitment potencies.

EC50 were determined, as described in *Materials and Methods*. Data shown are the mean ± S.E.M. of three independent experiments.

Receptor expressed	Log EC50 (M)
WT-V2R	-9.44 ± 0.09
R137H-V2R	-9.53 ± 0.12
R137C-V2R	-9.34 ± 0.19
R137L-V2R	-9.64 ± 0.17

Molecular Pharmacology Fast Forward. Published on February 16, 2010 as DOI: 10.1124/mol.109.061804
This article has not been copyedited and formatted. The final version may differ from this version.

Figure 1

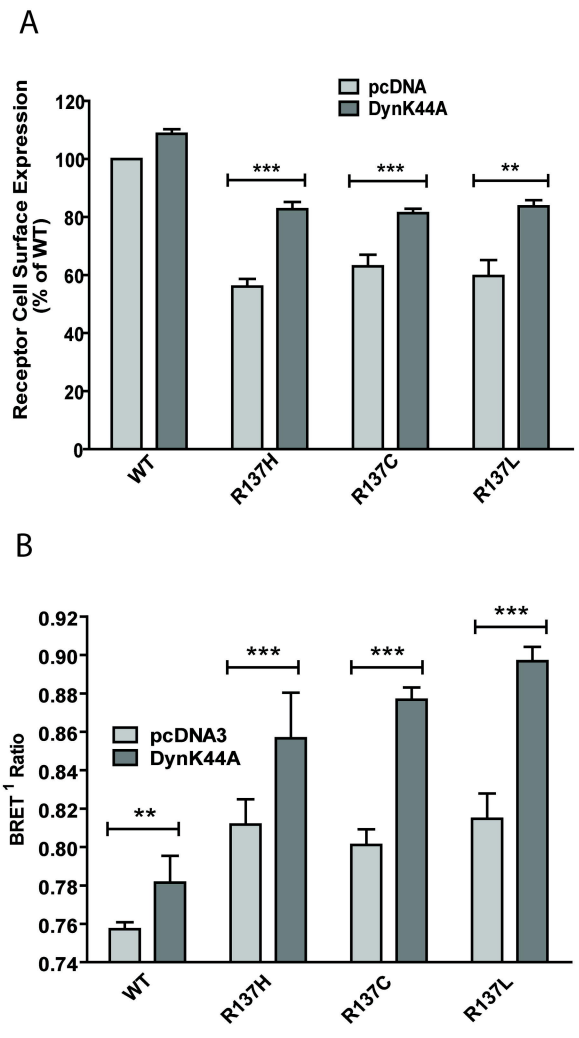

Molecular Pharmacology Fast Forward. Published on February 16, 2010 as DOI: 10.1124/mol.109.061804
This article has not been copyedited and formatted. The final version may differ from this version.

Figure 2

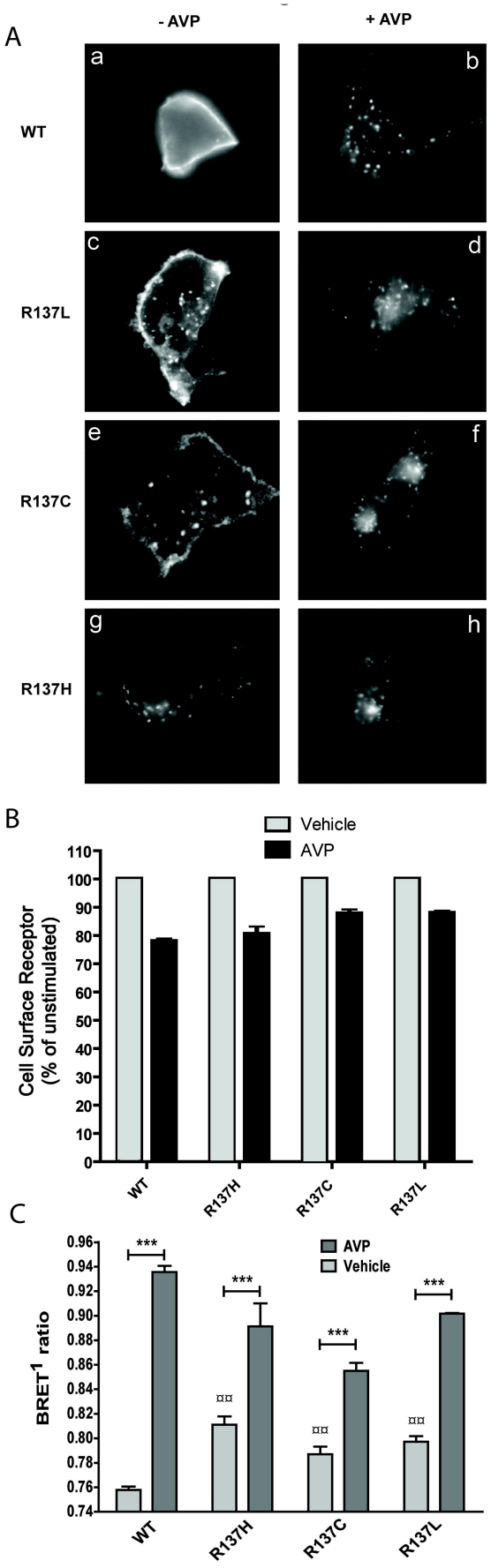

Molecular Pharmacology Fast Forward. Published on February 16, 2010 as DOI: 10.1124/mol.109.061804
This article has not been copyedited and formatted. The final version may differ from this version.

Figure 3

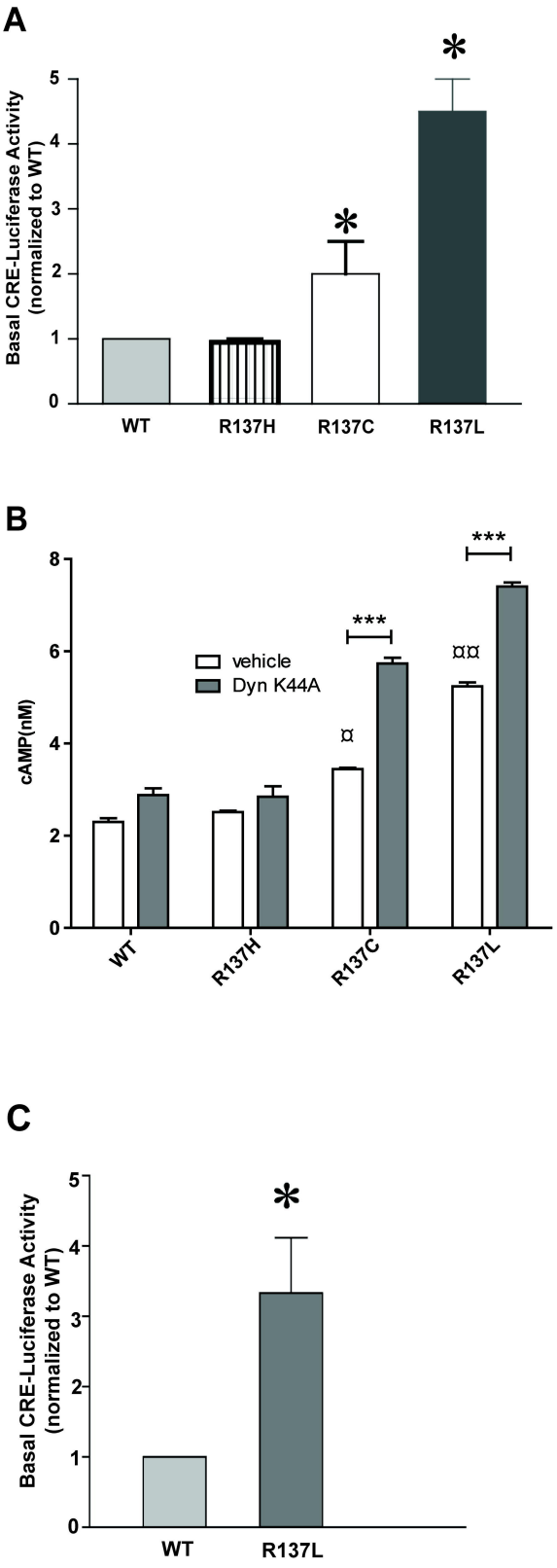

Molecular Pharmacology Fast Forward. Published on February 16, 2010 as DOI: 10.1124/mol.109.061804
This article has not been copyedited and formatted. The final version may differ from this version.

Figure 4

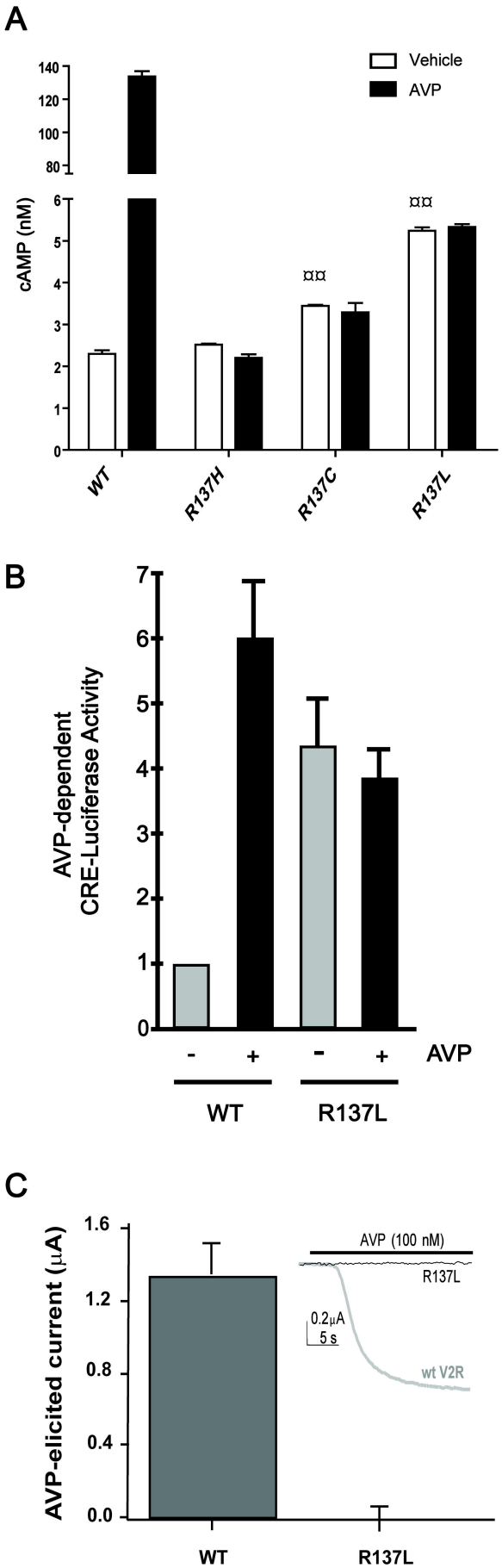

Molecular Pharmacology Fast Forward. Published on February 16, 2010 as DOI: 10.1124/mol.109.061804
This article has not been copyedited and formatted. The final version may differ from this version.

Figure 5

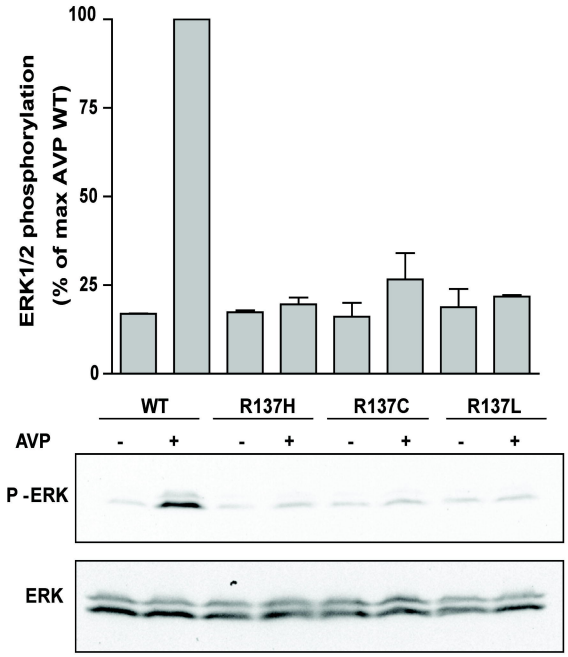

Molecular Pharmacology Fast Forward. Published on February 16, 2010 as DOI: 10.1124/mol.109.061804
This article has not been copyedited and formatted. The final version may differ from this version.

Figure 6

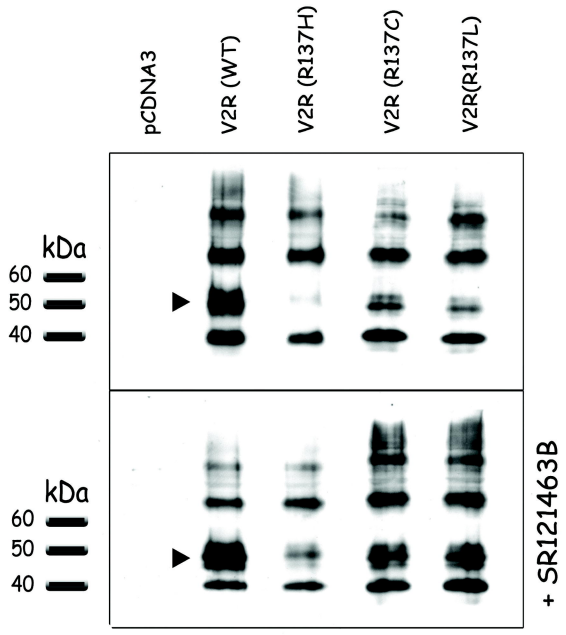

Molecular Pharmacology Fast Forward. Published on February 16, 2010 as DOI: 10.1124/mol.109.061804
This article has not been copyedited and formatted. The final version may differ from this version.

Figure 7

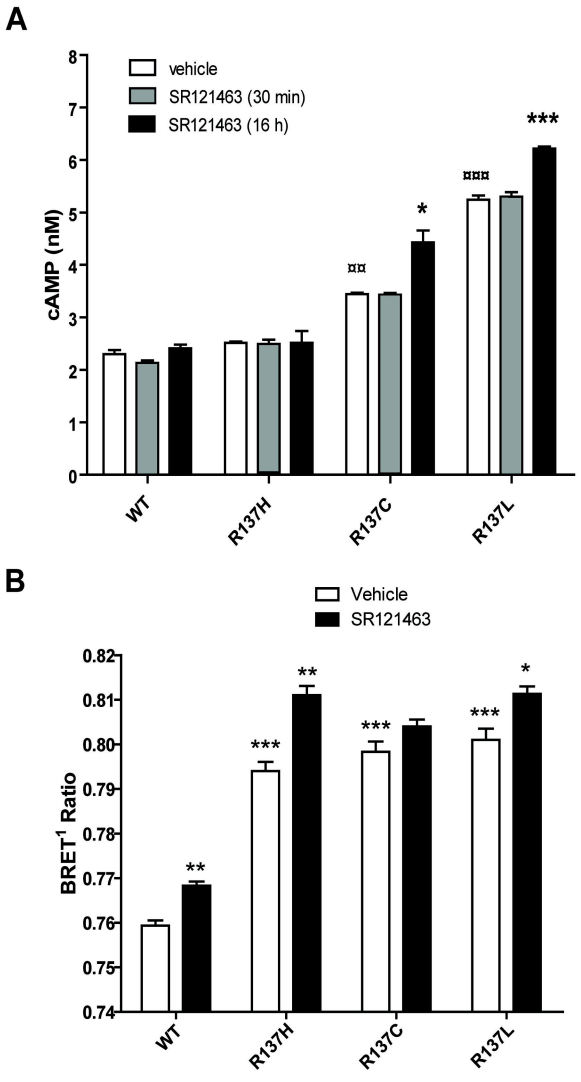

Molecular Pharmacology Fast Forward. Published on February 16, 2010 as DOI: 10.1124/mol.109.061804
This article has not been copyedited and formatted. The final version may differ from this version.

Figure 8